Journal of Applied Fluid Mechanics, Vol. 16, No. 12, pp. 2300-2315, 2023.
Available online at www.jafmonline.net, ISSN 1735-3572, EISSN 1735-3645.
https://doi.org/10.47176/jafm.16.12.2030

Numerical Study of Forced Nonlinear Acoustic Gas Oscillations in a Tube under the Action of Two Pistons with Phase Shift

D. A. Gubaidullin and B. A. Snigerev †

Institute of Mechanics and Engineering, FRC Kazan Scientific Center, Russian Academy of Sciences, ul. Lobachevskogo 2/31, Kazan, Tatarstan, 420111, Russia

†*Corresponding Author Email: snigerev@imm.knc.ru*

ABSTRACT

Nonlinear acoustic oscillations of large amplitude created in a gas-filled tube under the action of two pistons located at the ends of the pipe are numerically investigated. The pistons oscillate according to the harmonic law at one of the natural frequencies and with different values of phase shift. The movement of the gas is described by mathematical equations of conservation for the main determining relations for the flow, which are estimated by applying the finite volume method based on OpenFOAM package. The non-stationary forced oscillatory motion of a gas inside an axisymmetric tube from a state of rest to a periodic steady motion is investigated. The features of nonlinear acoustic fluctuations of gas in cylindrical duct under the action of two pistons are found. The effect of the phase shift value has a strong effect on the oscillation amplitude of gas, when pistons oscillating at equal natural frequencies, in turn, when the pistons oscillate at different natural frequencies, the effect is very small. In particular, resonant oscillations are detected when the pistons vibrate at the same frequency values equal to odd values of their own higher harmonics in the absence of a phase shift value. In the case when the frequency values are equal to even values of the natural harmonics, resonant oscillations occur when the pistons move in anti-phase. The numerical method appears to work well and would be hoped for practical computations of different resonators.

Article History

Received May 26, 2023
Revised August 11, 2023
Accepted August 21, 2023
Available online October 8, 2023

Keywords:

Closed acoustic resonator
Nonlinear standing wave
Finite volume method
Weak shock wave
Navier-Stokes equations

1. INTRODUCTION

Creating intense pressure oscillations inside channels has a variety of practical applications in many areas of technology, ranging from acoustic compressors (Backhaus & Swift, 1999), thermal acoustic devices (Thomas & Muruganandam, 2018), to engines (Swift, 1992). Since the performance of such devices increases with the increase in the intensity of forced pressure fluctuations, the scientific researchers continue to search for new approaches and methods to increase the amplitude of acoustic harmonic oscillations and methods for their control. A large number of theoretical, numerical, and experimental papers have been devoted to the study of oscillations in tubes (Saenger & Hudson, 1960; Chester, 1963; Aganin et al., 1996; Cruikshank, 1972; Zaripov & Ilhamov, 1976; Alexeev & Gutginger, 2003; Hossain et al., 2005; Penelet et al., 2012; Antao & Farouk, 2013; Ning & Li, 2013; Pillai & Manu, 2020). Most of these works are devoted to the study of straight cylindrical channels with a solid rigid wall at one end and a movable piston at the other. The vibration of the piston near the resonant frequency for the tube leads to the formation of vibrations of the gas column inside the channel with a more intense oscillation amplitude. Early studies have shown that an increase in the amplitude of the piston movement at the frequency that characterizes the maximum response leads to the formation of pressure waves with a steep frontal front (saw-tooth) inside the resonator. One way to increase the amplitude of harmonic oscillations is to use a resonator with a variable cross-sectional area, as opposed to straight cylindrical channels (Lawrenson et al., 1998). In a number of works, numerical methods based on the finite-difference approach are used to study one-dimensional oscillations in the channels (Ilinskii et al., 1998; Chun & Kim, 2000; Vanhille & Campos-Pozuelo, 2001). Acoustic effects are used in various process reactors for the chemical industry. In order to develop the most economical modes of use of these devices, it is desirable to make a preliminary assessment of productivity and efficiency at operation at various determining mode parameters, selection of the most suitable operating media. The most accurate prediction for determining economical modes can be obtained with the help of three-dimensional mathematical modeling based on equations that adequately describe all the processes taking place. The developed numerical algorithms and computational software packages using the basic laws of

NOMENCLATURE

c_p	heat capacity of air	t	time
d_0	diameter of the tube	ρ	density of air
L	length of the tube	η	dynamic viscosity of air
k	thermal conductivity of the air	τ_{ij}	viscous stress tensor
M_{ac}	Mach number	δ_v	acoustic boundary layer thickness (viscous penetration depth)
Pr	Prandtl number	ϕ	phase angle
Re_{ac}	acoustic Reynolds number	OpenFOAM	open field operation and manipulation
u_i	velocity components (i=1, 2, 3)	FFT	fast Fourier transform
ω	angular frequency of oscillation	CFD	computational fluid dynamics
T	static temperature	CFL	Courant Friedrichs Lewy

conservation of mass, angular momentum and energy are increasingly widely used for these purposes (Marie et al., 2009). The use of forced oscillations in various branches of industry is constantly expanding, generated by external influences. In thermoacoustic systems with many plates inside the resonator, which narrow the flow area, turbulent pulsations can occur in the vicinity of these baffles. The software packages modeling spatial flows with different turbulence models are being actively developed for modeling such flows. The state of the art and the tremendous progress that has been made in hybrid modeling of aero-acoustic sound are reviewed in (Colonius & Lele, 2004; Wang et al., 2006). The usage of OpenFOAM for different aeroacoustics problems is demonstrated in (Singh & Rubini, 2015; Piscaglia et al., 2013). The different usage of solver from this software package for modeling gas fluctuations in a cylindrical duct, accompanying by the formation of standing waves with sharp crests are presented in (Gubaidullin & Snigerev, 2022). Here nonlinear characteristics for heavy fluctuations of compressible gas in a closed duct at higher natural frequency have been found. For non-linear gas fluctuations with a weak shock wave of pressure drop in the nodes for the velocities, the extensive amplitudes of the alterations in particle velocities over a very small interval of time are generated. Many works have been devoted to the experimental and theoretical study of flows caused by vibrations of cylinders or bluff bodies, which is reflected in the review (Wang et al., 2020). Various important phenomena of interaction between liquids and oscillating bodies have been identified, depending on the different modes of their oscillations. The effect of the phase shift of the oscillations of two twin square cylinders on the flow structure was carried out in (Mithun et al., 2018). The improvement of the heat exchange processes of the oscillating plate inside the cylinder was carried out in (Li et al., 2016). Theoretically and experimentally, the peculiarity of the flow near oscillating square cylinders in the form of an effect the 'lock-in' phenomena, where the vortex shedding becomes one with the oscillation frequency, is observed (Bearman & Obasaju, 1982).

For more better understanding of the features of acoustic flows, studies of acoustic gas oscillations in resonators arising from forced excitations under the influence of several phase-shifted pistons become relevant. In this study, the goal is to examine propagation of acoustic waves in cylindrical duct under the action of two movable pistons at both ends at first natural frequency and for higher garmonics. The features of acoustic gas oscillations during piston vibrations at equal natural frequencies with a phase shift and also at different values of the natural harmonics are considered. For those values of phase shift of pistons oscillations when resonant oscillations of gas in the tube occur, informative waveforms of pressure and particle velocity variations along the center of the duct for one oscillation period are presented . To solve this problem, a numerical method has been used for modeling nonlinear acoustic spatial resonators under the influence of complex harmonic excitation with phase shift. To approximate the equations describing the motion of a viscous heat-conducting gas, the technology of the OpenFOAM library is used, when the relations written in integral form valid for the selected control volume of the region are discretized (Weller et al., 1998; Moukalled et al., 2001). The solver *rhoPimpleCentralFoam* developed in (Kraposhin et al., 2015; Kraposhin et al., 2018) is used, which is designed to model gas flows over a wide range of the velocities. The propagation of waves back and forth in a tube is generated by two movable pistons at the ends. Weak shock waves propagating within the tube at the first resonant frequency and higher modes frequencies are numerically captured.

The remaining material of the article is planned in the following paragraphs. In Sec. II the Navier-Stokes for compressible gas are presented. The results of numerical simulation of fluctuations of gas in duct forced by two pistons vibrating at different natural harmonics with phase shift are presented in Sec. III. Finally, the conclusions of the paper are given in Sec. IV.

2. MATHEMATICAL MODEL

The mathematical model based on our previous study (Gubaidullin & Snigerev, 2022), where nonlinear acoustics forced oscillations in gas-filled tube, created by one piston are investigated. The used numerical model give results which are in good agreement with the data for intensive gas oscillations with breaking waves of various experiments (Saenger & Hudson, 1960; Zaripov & Ilhamov, 1976; Alexeev & Gutginger, 2003) and numerical research (Antao & Farouk, 2013). An extended description of the numerical model using the OpenFOAM library (Moukalled et al., 2001) is given in (Gubaidullin & Snigerev, 2022), and this paper gives only a brief description of the used numerical method. The flow and heat transfer modelling include the fluid dynamic equations of conservation of mass (continuity equation),

momentum (Navier-Stokes equation), and energy for considered domain. They written in cartesian form as:

$$\frac{\partial \rho}{\partial t}+\frac{\partial(\rho u_i)}{\partial x_i}=0, \tag{1}$$

$$\frac{\partial(\rho u_j)}{\partial t}+\frac{\partial(\rho u_j u_i)}{\partial x_i}=\frac{\partial P}{\partial x_j}+\frac{\partial \tau_{ji}}{\partial x_i}, \tag{2}$$

$$\tau_{ji}=\mu\left(\frac{\partial u_j}{\partial x_i}+\frac{\partial u_i}{\partial x_j}\right)-\frac{2}{3}\mu\frac{\partial u_k}{\partial x_k}\delta_{ji}, \tag{3}$$

$$c_p\frac{\partial(\rho T)}{\partial t}+c_p\frac{\partial(\rho u_i T)}{\partial x_i}-\frac{1}{\rho}\left(\frac{\partial(\rho p)}{\partial t}+\frac{\partial(\rho u_i p)}{\partial x_i}\right) = \frac{\partial}{\partial x_i}\left(k\frac{\partial T}{\partial x_i}\right)+\tau_{ij}\frac{\partial u_j}{\partial x_i} \tag{4}$$

The equation of state was choosing as $p=\rho RT$, where R universal gas constant. It is assumed that the thermo-physical properties η and k related on temperature. The dynamic viscosity η is specified by Sutherland law

$$\frac{\eta}{\eta_0}=\left(\frac{T}{T_0}\right)^{1.5}\frac{T_0+C}{T+C}, \tag{5}$$

where $T_0=273$ K, $\eta_0=1.789\times10^{-5}$ Pa s, C is constant with value 110. The following relation is applied for thermal conductivity $k=\frac{\eta c_p}{\mathrm{Pr}}$, $\mathrm{Pr}=0.72$. The accurate representation of gas behavior by equations (1) - (5) are solved by means of solver, which based on the open source CFD toolbox OpenFOAM (Weller et al., 1998; Moukalled et al., 2001). A full description of the numerical methodology is presented in a previous paper (Gubaidullin & Snigerev, 2022).

3. RESULTS AND DISCUSSION

The scheme of computational domain used for numerical simulation is shown on Fig. 1. The area is represented by a duct, which has a length $L=6.567\cdot10^{-3}$ m with diameter $d_0=28\cdot10^{-3}$ m. On left side ($x_1=L$), the tube is closed the left end by a piston that oscillates according to the law $x_1^L=l_0\sin\left(\omega^L t+\phi^L\right)$, and on the other side with another piston with moving as $x_1^R=l_0\sin\left(\omega^R t+\phi^R\right)$. The pistons movement amplitude is $l_0=33\cdot10^{-3}$ m. Non-dimensional parameter for the selected tube $\varepsilon=\left(\pi l_0/L\right)^{1/2}$ is 0.126. The pressure ($p_0=101325$ Pa), density ($\rho_0=1.165$ kg/m^3), temperature ($T_0=293$ K) taken for air at standard thermodynamic conditions. The rest parameters are taken as: the gas constant $R=287$ J/kg K, specific heat at constant pressure $C_p=1.006$ kJ/ kg K , the speed of sound is defined as $c_s=\left(\gamma RT_0\right)^{1/2}$. To determine the nature of the oscillations in the resonator, we introduce four control points (1, 2, 3, 4), which is located in coordinates 1- $x_1/L=0.02$, 2- $x_1/L=0.5$, 3- $x_1/L=0.75$, 4- $x_1/L=0.98$ (Fig. 1). The control points 1, 4 are located in the area close to the end walls of the resonator, and the point 2 corresponds to the middle of the pipe, the point 3 corresponds to the middle of second half of the tube. In the case of linear oscillations, these points are characteristic of oscillations at the first natural frequency (the pipe length is $L=\lambda/2$). The point located in the center of the pipe is the node for pressure (minimum amplitude of oscillations), and the extreme points are anti-nodes (maximum amplitude). The viscous penetration depth for oscillations flow is given by $\delta_v=\sqrt{\frac{2\eta}{\rho\omega}}$ (Kinsler et al., 1999). Dimensionless characteristic parameters local acoustic Reynolds and Mach number defined as (Kinsler et al., 1999; Antao & Faraok, 2013)

$$\mathrm{Re}_{ac}=\frac{U_0\delta_v\rho}{\eta},\quad M_{ac}=\frac{U_0}{c_s} \tag{6}$$

Use the value for U_0 the meaning of $u_1^{\max}$, where $u_1^{\max}$ is the largest velocity value in duct for oscillations in the tube (obtained from calculation on coarse grid) the maximum acoustic Reynolds and Mach numbers take the values $\mathrm{Re}_{ac}^{\max}=597$, $M_{ac}^{\max}=0.14$. The issue of transition from the laminar stream to unstable regime for oscillating flows, with the possible formation of turbulent pulsations is discussed in (Ohmi & Iguchi, 1982; Carpinlioglu & Gundogdu, 2001). The velocity $\mathrm{Re}_{ac}^{\max}$ calculated from the maximum velocity value is in the range of values for the laminar flow regime, according to the estimates proposed in (Carpinlioglu & Gundogdu, 2001). Hence for the description the oscillations of gas in the tube, the unsteady Navie-Stokes equations (1) - (4) can be used. Forced acoustic oscillations of a gas column with piston moving by at one end of resonator induce a high-amplitude standing wave on resonant frequencies

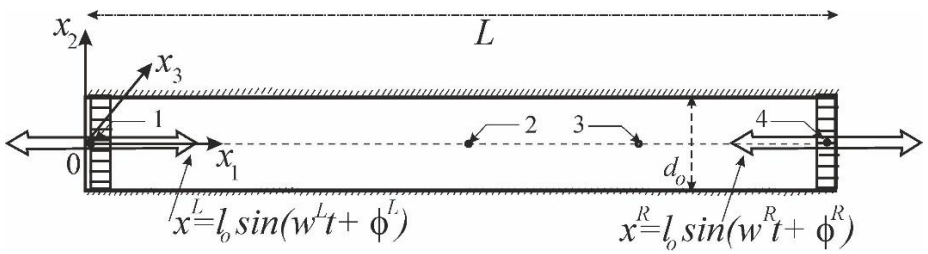

Fig. 1 Model of resonator with two pistons

$$\omega_n = n\pi c_s / L, \qquad n = 1, 2, \ldots \tag{7}$$

where c_s is the speed of sound in the undisturbed flow. In the case of excitation of oscillations by means of two pistons at resonant frequencies, defined for a pipe with one closed end by the relation Eq. (7), acoustic flow depends from the parameters, determining the frequency ω and phase shift ϕ given at the opposite ends of the tube. The system under consideration is a gas-filled tube (Fig. 1), closed at the left end by a piston that oscillates according to the different laws as $x_1^L = g\left(\omega_i^L, \phi_j^L\right) = l_o \sin\left(\omega_{i=1,..4}^L t + \phi_j^L\right)$, where $\omega_{i=1,..4}^L$ takes the values $\omega_1, \omega_2, \omega_3, \omega_4$, and the value of φ_j^L parameter remains unchanged as $\phi^L = 0$. On the right end, the piston oscillates according to the law, which has the form $x_1^R = g\left(\omega_i^R, \phi_j^R\right) = l_o \sin\left(\omega_{i=1,..4}^R t + \phi_j^R\right)$, on the right piston ω_i^R updates similarly to ω_i^L and the phase shift ϕ_j^R can take the following values $\phi_{j=1,..4}^R = \pm j \times \frac{\pi}{4}$ for equal frequencies, and $\phi_{j=1,..4}^R = 0,\ \pi/3,\ \pi/2,\ \pi$ for non-equal frequencies. Therefore, the calculations for the selected two variants of piston parameters change are given below. For the first variant the same values of frequencies for both pistons are considered, and for the second case at different values of piston motion parameters with phase shift.

3.1 Movement of Pistons at Equal Resonant Frequencies with Phase Shift

a) *Oscillations at first resonant frequency* $\omega^L = \omega^R = \omega_1$. Consider first the case of oscillations when oscillations occur with equal resonance frequencies on the left and right piston, in this event, the frequencies coincide with the first resonant harmonics $x_1^L = g\left(\omega_1, \phi^L\right)$, $x_1^R = g\left(\omega_1, \phi^R\right)$. On the left piston $\phi^L = 0$, and on the right piston, the phase shift ϕ^R changes for each case with increments $\frac{\pi}{4}$, $\phi_j^R = j \cdot \frac{\pi}{4},\ j = \pm 1, ..4$. The time, when the structure will make 80 ($t c_s / 2L = 80$) oscillation cycles is selected for presentation of calculation results at the first mode. Gas fluctuations in a circular tube are assumed to be axisymmetric, so as the computational domain the part of the duct with the solution angle 5 is selected, as shown in Fig. 2. In the numerical solution of equations (1) - (5), boundary conditions of symmetry are set on the side walls of the selected sector. The movement of the piston is given as a boundary condition in the form as $u_1^L = d\, x_1^L / dt = l_0\, \omega_1^L \cos\left(\omega_1^L t + \phi^L\right)$. The boundary conditions are given on the input wall S_1: $u_1^L = l_0\, \omega_1^L \cos\left(\omega_1^L t + \phi^L\right)$, $u_2, u_3 = 0$, $T = T_0$, $p = p_0$. On the right piston the boundary conditions are applied similar way as $u_1^R = l_0\, \omega_1^R \cos\left(\omega_1^R t + \phi^R\right)$, $u_2, u_3 = 0$, $T = T_0$, $p = p_0$. On the wall of the duct S_5 "no-slip"

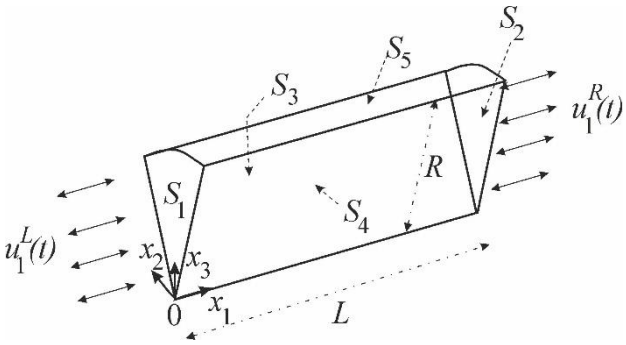

Fig. 2 Sketch of computational domain for axisymmetric model of gas oscillations in cylinder tube with two pistons

conditions $u_i = 0, (i = 1..3)$ and $\partial T / \partial n = 0$ are imposed. On the left S_3 and right S_4 boundary of the selected sector of tube:

$$\frac{\partial p}{\partial n} = 0, \quad \frac{\partial \rho}{\partial n} = 0, \quad \frac{\partial u_s}{\partial n} = 0, \quad \frac{\partial T}{\partial n} = 0, \quad u_n = 0,$$

where n is the normal, and s is the tangent unit vectors to the surface. Initial conditions taken as $u_i = 0,\ p = p_o, T = T_0, \rho = \rho_0$, with being ρ_0, p_0 and T_0 are properties of air at standard thermodynamic conditions.

The numerical scheme is tested for convergence on grids with different mesh sizes including finite volumes M_e =34560, 138240, 276480. On plane side S_3 faces of volumes are rectangles with divisions in directions x_1 and x_2 for different meshes are $N_1 = 512 \times 64$, $N_2 = 1028 \times 128$, $N_3 = 2056 \times 128$. For mesh N_2 the face of surface S_3 was separated into 1028 grid points with equal size $h_{x_1} = 3.32 \times 10^{-3}$ m in axial direction x_1 . In direction x_2 the rectangles are compressed in the direction of the solid wall. The viscous penetration depth have value $\delta_v = 3.08 \times 10^{-4}$ m. Near the wall at a depth of δ_v there are 5 computational grid nodes, so that the largest and the smallest mesh size are $h_{x_2}^{\max} = 6.8 \times 10^{-4}$ and $h_{x_2}^{\max} = 6.8 \times 10^{-4}$ m respectively. The calculations are performed with time step Δt , which satisfies the CFL condition with a Courant number ($C = \left(c_s \times \Delta t\right) / \Delta x$, where c_s is the acoustic speed for air, $\Delta x = \min\left(h_{x_1}, h_{x_2}, h_{x_3}\right)$) is equal to 0.4. For mesh N_2 , Δt is taken to be 1.12×10^{-5} s. In Fig. 3 the numerical convergence with number of control volumes increasing is examined for the case $x_1^L = g\left(\omega_1, 0\right)$, $x_1^R = g\left(\omega_1, \pi/2\right)$. The pressure and axial velocity in some control points of the tube are obtained on three different grids of N_1, N_2, N_3 . On Fig. 3(a) it is shown that difference in distributions of pressure on variation of meshes is very small. The alterations of velocity $u_1 / \omega l_0$ at central point2 with time $t c_s / L$ are demonstrated on Fig. 3(b).

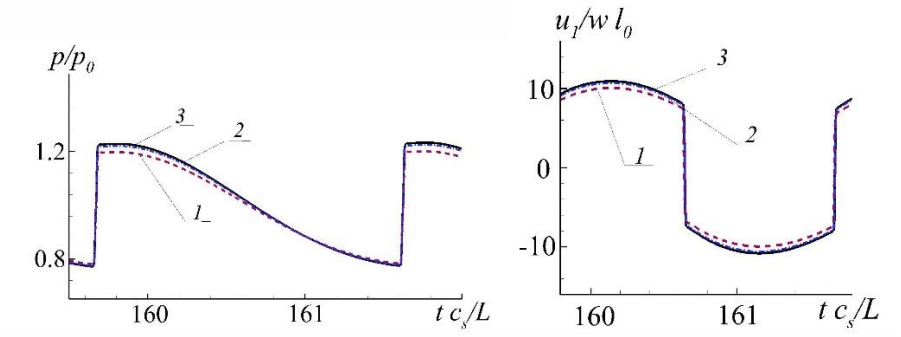

(a) (b)

Fig. 3 Mesh refinement study (curve 1 - N_1 mesh, 2 - N_2, 3 - N_3) of the time dependent on the dimensionless time tc_s/L for $x_1^L=g(\omega_1,0)$, $x_1^R=g(\omega_1,\pi/2)$ variables: (a) p/p_0 at point 1($x_1/L=0.02$); (b) axial velocity component $u_1/\omega_1 l_o$ at point 2 ($x_1/L=0.5$)

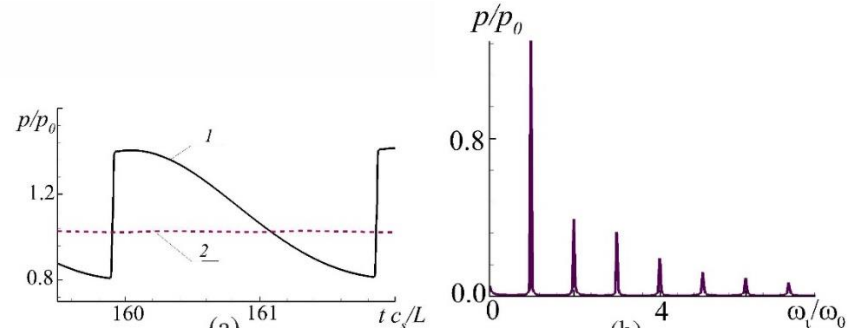

(a) (b)

Fig. 4 (a) Time dependences for $x_1^L=g(\omega_1,0)$, $x_1^R=g(\omega_1,\phi_{j=1,2}^R)$ at point 1 on the dimensionless time tc_s/L variable p/p_0 for different values of phase shift ϕ^R : curve 1- $\phi^R=0$, $\phi^R=\pi$; (b) Fourier transform of the signal p/p_0 in time at point 1 for $\omega^L=\omega^R=\omega_1,\phi^L=\phi^R=0$

The feature of nonlinear vibrations are manifested by the fact, that vertical velocity jumps occur at some time instant at nodal point for the oscillation velocity. The grid N_2 provides satisfactory accuracy for the calculations, therefore it is chosen as the base grid for the computations. The Fig. 4(a) shows the dynamics of the pressure change over dimensionless time values tc_s/L from 160 to 162 at point 1 for cases when the pistons oscillate at the first resonant frequency ($x_1^L=g(\omega_1,0)$, $x_1^R=g(\omega_1,\phi_{j=1,2}^R)$) with two phase shifts on the right piston $\phi_{j=1,2}^R=0,\pi$. In Fig. 4(a), curve 1 corresponds to the case when $\phi^L=0,\phi^R=0$, and curve 2 - $\phi^L=0,\phi^R=\pi$. Analysis of this figure indicates that in the case of piston oscillations without phase shift (Fig. 4(a), curve-1), the oscillations are superimposed on both pistons and, over time, intense resonance oscillations develop with a weak shock front in the tube. In case of $\phi^R=\pi$ (Fig. 4(a), curve-2) the opposite effect occurs, leading to practical damping of oscillations at the left end, and in the whole area of the tube. The maximum values of the pressure drop at point 1 correspond to the linear theory, according to which, there is an antinode of pressure where it transforms from time to time according to the harmonic law with a large amplitude. For strong nonlinear oscillations, it can be seen that the pressure profile is very different from the harmonic character, since the pressure wave profile is not symmetrical with respect to the central axis relating to the external atmospheric pressure. The left part of the pressure front has a steep vertical section of the pressure increase, and the right part of the pressure decrease is more smooth. The Fig. 4(b) presents the FFT of the pressure time history p/p_0 at point 1 for the case $\omega^L=\omega^R=\omega_1,\phi^L=\phi^R=0$ at the resonant frequency, p/p_0 is the non-dimensional oscillating pressure. It can be seen that in this case, the resonant oscillations are observed at the first resonant frequency. The pressure drop $\Delta p^*=(p_{\max}-p_{\min})/p_0$ drops from a value of 0.65 to 0.03. The Fig. 4(b) shows that the pressure change over time, has the largest amplitude at the first harmonic, and the amplitudes of the other higher harmonics monotonically decrease with increasing values of the multiplicity of the natural frequency. The Fig. 5 illustrates similar curves corresponding to the midpoint of the duct (point 2) for the same time period. For this point, according to the linear theory, corresponding to the pressure node ($\omega=\omega_1, L=\lambda/2$), the resonant pressure fluctuations

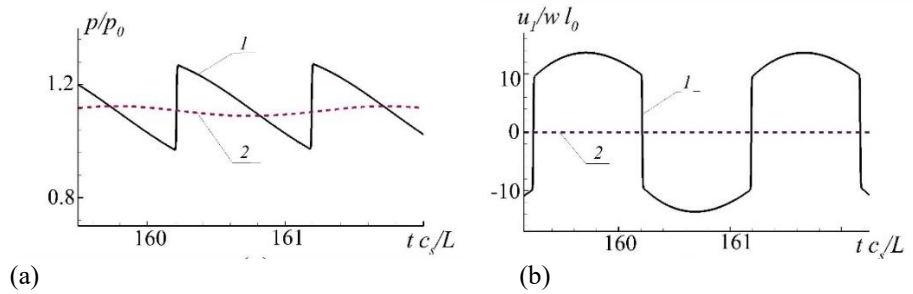

Fig. 5 (a) Time dependences for $x_1^L = g(\omega_1, 0)$, $x_1^R = g(\omega_1, \phi_{j=1,2}^R)$ at point 2 on the dimensionless time tc_s/L variable p/p_0 for different phase shift $\phi_{j=1,2}^R$ values: 1- $\phi^R = 0$, 2- $\phi^R = \pi$; (b) the axial component of the velocity $u_1/\omega_1 l_0$ at different value of $\phi_{j=1,2}^R$: 1- $\phi^R = 0$, 2- $\phi^R = \pi$

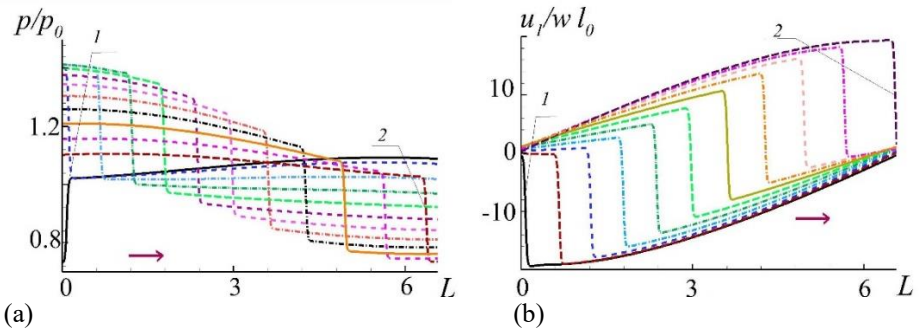

Fig. 6 Axial variations of variables for $x_1^L = g(\omega_1, 0)$, $x_1^R = g(\omega_1, 0)$ with a time increment of $\Delta tc_s/L = 0.1$ for half-period of oscillations for dimensionless time tc_s/L from 160 to the 161: (a) pressure p/p_0 ; (b) axial velocity component $u_1/\omega_1 l_0$

should be minimal. In the case of nonlinear oscillations, it can be observed that p/p_0 is about half of the values from point 1, and the oscillation frequency is twice of the resonant frequency ($\omega = 2\omega_1$, Fig. 5(a)). The shape of the pressure waves in this case has a saw-shaped character, containing a vertical section of pressure growth, and an almost linear section of decrease, and there is no smooth transition between them. Intense vibrations of the axial velocity in the middle of the tube (point 2) is illustrated in Fig. 5(b) (curve - 1). A special feature of the velocity allocation is the transition from sinusoidal forms of velocity change over time with harmonic oscillations to almost rectangular forms, when the smooth alteration is replaced by a jump-like one with some smooth section for changing the direction of the speed from positive to negative. Similar calculations for the resonator at the first resonant frequency of both pistons at shift parameters values of $\phi^L = 0$, ϕ^R updates for right piston from $\phi^R = 0$ to $\phi^R = \pi$ with step $\Delta\phi^R = \pi/4$ showed, that at $\phi^R = 0$ the oscillations of gas are resonant, and by increasing the phase shift parameter ϕ^R the oscillations intensity decreases, until $\phi^R = \pm\pi$, when the oscillations almost damped. The Fig. 6 shows the instantaneous waveforms of pressure and velocity along the coordinate x_1 ($0 \le x_1 \le L, x_2, x_3 = 0$) for one cycle of oscillations for corresponding time 160 to 161 with time step $\Delta tc_s/L = 0.1$ for $x_1^L = g(\omega_1, 0)$, $x_1^R = g(\omega_1, 0)$. In this picture, the number 1 marks the curve showing the pressure waveforms at time instant, when the maximum pressure drop is located near the left piston, and the number 2 corresponds to the state when the pressure peak reaches the opposite end of the pipe, moving in the direction shown by the arrow. The first half of the fluctuation period is characterized by the fact, that the zone of increased pressure, created by the left piston moves through the tube with a monotonous decrease in the maximum value as it approaches to the right piston. The amplitude of pressure fluctuations as it moves is preserved, and after reflection from the right piston the dynamics of pressure changes occur in the opposite direction. The movement of the pressure drop along the duct (Fig. 6(a)) is accompanied by a change of the velocity $u_1/\omega l_0$ along the coordinate x_1 ($0 \le x_1 \le L, x_2, x_3 = 0$), shown in Fig. 6(b). The propagation of a weak pressure shock wave along the duct leads to the fact, that it is accompanied by movement of the zone of strong change of particle velocities in the same direction. The movement of the pistons at the first harmonic with a phase shift leads to an increase in the amplitude of oscillations and the formation of resonance only for the case $x_1^L = g(\omega_1, 0)$, $x_1^R = g(\omega_1, 0)$. With the change of ϕ^R a monotonic decrease of the oscillation amplitude is observed, and at $x_1^L = g(\omega_1, 0)$, $x_1^R = g(\omega_1, \pi)$ the there is a significant damping of oscillations in the whole tube region.

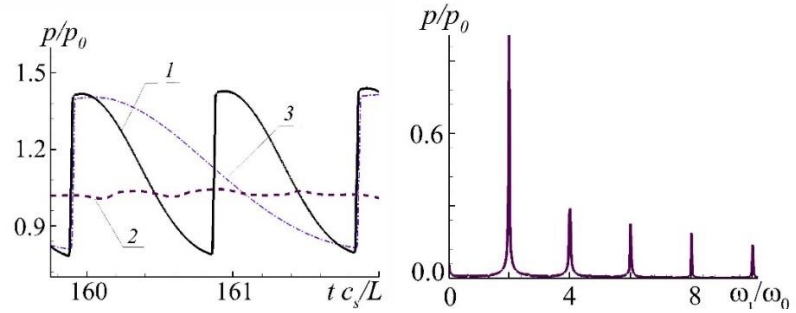

(a) (b)

Fig. 7 (a) Time dependences for $x_1^L=g(\omega_2,0)$, $x_1^R=g\left(\omega_2,\phi_{j=1,2}^R\right)$ at point 1 on the dimensionless time tc_s/L variable p/p_0 for different values of phase shift ϕ^R curve 1- $\phi^R=\pi$, 2- $\phi^R=0$;3- $x_1^L=g(\omega_1,0)$, $x_1^R=g(\omega_1,0)$; (b) Fourier transform of the signal p/p_0 in time at point 1 for $x_1^L=g(\omega_2,0)$, $x_1^R=g(\omega_2,\pi)$

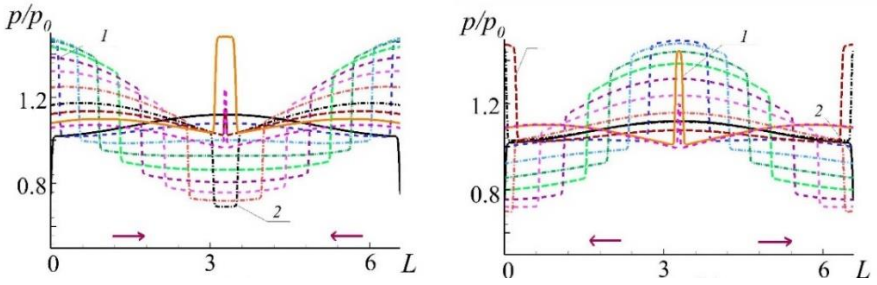

(a) (b)

Fig. 8 Axial variations of pressure p/p_0 for $x_1^L=g(\omega_2,0)$, $x_1^R=g(\omega_2,\pi)$ along center line with a time increment of $\Delta tc_s/L=0.07$: (a) for first half-period of oscillations with dimensionless time tc_s/L from 160 to the 160.5; (b) for second half-period of oscillations from time 160.5 to the 161

b) Oscillations at second resonant frequency $\omega^L=\omega^R=\omega_2$. A similar oscillation mode behavior depending on the phase shift was found at the second resonant frequency $x_1^L=g(\omega_2,0)$, $x_1^R=g\left(\omega_2,\phi^R\right)$ for both pistons. On the left piston $\phi^L=0$, and on the right piston, the phase shift changes for each case with increments of $\frac{\pi}{4}$, $\phi_j^R=j\cdot\frac{\pi}{4}$, $j=\pm1,..4$. Some own features in behavior of oscillations the gas in tube are found. The Fig. 7(a) presents the dynamics of the pressure change over time at point 1 for cases when the pistons oscillate at the second resonant frequency ($\omega^L=\omega^R=\omega_2$) with two phase shifts on the right piston $\phi_{j=1,2}^R=0,\pi$. In this case, the boundary conditions do not update, except for the frequency of forced oscillations on both pistons are doubled ($\omega^L=\omega^R=\omega_2=2\omega_1$). Comparing Fig. 4(a) and Fig. 7(a) it can be observed, that if at the first natural frequency resonant oscillations are formed at $\phi^R=0$, then at the second harmonic the behavior is exactly the opposite. At an even second harmonic, the resonant response occurs at $\phi^R=\pi$, and at the $\phi^R=0$ oscillations are damped. In this case, the maximum value of the pressure drop increases by 2% percent, and the attenuation also occurs with an increased amplitude of about 9 % percent, while the speed and frequency of the piston movement are doubled. The Fig. 7(b) presents the FFT of the pressure time history of p/p_0 at point 1 for the case $\omega^L=\omega^R=\omega_2$, $\phi^R=\pi$. It can be viewed that in this case, resonant oscillations are observed at the second resonant frequency. The Fig. 7(b) shows that in the pressure change over time, the main component has the largest amplitude at the second harmonic, and the amplitudes of the other higher harmonics monotonically decrease with increasing values of the multiplicity to the second natural frequency. The Fig. 8 illustrates shows the instantaneous waveforms of pressure along the coordinate x_1 ($0\le x_1\le L, x_2, x_3=0$) for one cycle of oscillations for corresponding time 160 to 161 with step $\Delta tc_s/L=0.07$ for $x_1^L=g(\omega_2,0)$, $x_1^R=g(\omega_2,\pi)$. In Fig. 8(a), the number 1 marks the curve showing the pressure waveforms at time instant, when the two maximum pressure drops is located near the left and right piston, and the number 2 corresponds to the state, when the pressure peaks reaches the middle of the duct, moving in the directions shown by the arrows. Unlike to the first resonant frequency, when a single wave (Fig. 6(a)) propagates back and forth in the tube over time, two weak shock waves perform similar movements here. The Fig. 8(a) shows the convergence of two pressure drops towards the middle of the pipe, where the pressure is almost homogeneous and gradually decreases. The getting closer and then collision of two sharp pressure drops leads to their merging and the formation of one more powerful burst of pressure in a narrow zone, then it begins to spread in both directions with the formation of a new zone of uniform pressure in the middle of the duct (Fig. 8(b)). The

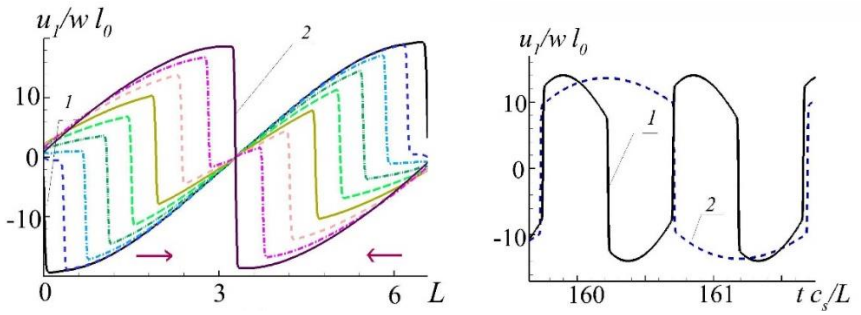

(a) (b)

Fig. 9 Variations of axial velocity component $u_1/\omega_1 l_0$ (a) along center line for $x_1^L=g(\omega_2,0)$, $x_1^R=g(\omega_2,\pi)$ with a time increment of $\Delta t c_s/L$=0.07 for first half-period of oscillations with dimensionless time tc_s/L from 160 to the 160.5; (b) time dependences $u_1/\omega_1 l_0$ on the time tc_s/L : 1- $x_1^L=g(\omega_2,0)$, $x_1^R=g(\omega_2,\pi)$ at point 3, 2 - $x_1^L=g(\omega_1,0)$, $x_1^R=g(\omega_1,0)$ at point 2

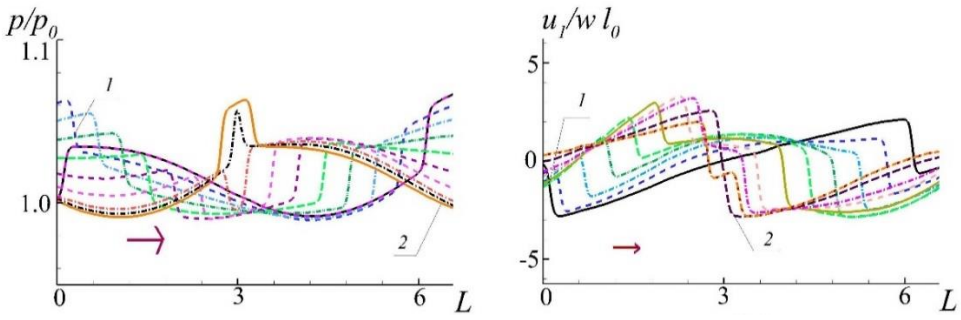

(a) (b)

Fig. 10 Axial variations of variables for $x_1^L=g(\omega_2,0)$, $x_1^R=g(\omega_2,\pi/10)$ with a time increment $\Delta t c_s/L$=0.07 of for half-period of oscillations for dimensionless time tc_s/L from 160 to the 161: (a) pressure p/p_0 ; (b) axial velocity component $u_1/\omega_1 l_0$

movement of the two pressure drops along the duct (Fig. 8(a)) is accompanied by a change the velocity $u_1/\omega l_0$ along the coordinate x_1 ($0\le x_1\le L, x_2, x_3=0$) as presented in Fig. 9(a). The unification and merger of two pressure drops in the middle of the duct caused to a sudden spike in pressure in the form of delta-function. The change in velocity near this section of the duct at a given time has the highest quantity (Fig. 9b, line 2). The variation of velocity in the vicinity of this area of the tube at this time instant has the maximum value. Within the second half-cycle of fluctuation, the slim area of excessive pressure begins to run away in the form of two pressure drop waves (Fig. 8(b)). The divergence of two differential pressures from the center of the pipe to the walls (Fig. 8(b)) leads to the dynamics of velocity distribution along the pipe axis similar to Fig. 9(a), except that the in this case the direction of movement of the narrow zones of the velocity drop is reversed. In Fig. 9(b) the time history of the velocity $u_1/\omega_1 l_0$ on the dimensionless time tc_s/L for $x_1^L=g(\omega_2,0)$, $x_1^R=g(\omega_2,\pi)$ at point 3, and for $x_1^L=g(\omega_1,0)$, $x_1^R=g(\omega_1,0)$ at point 2 are shown. Influence of the phase shift during gas fluctuations in the tube in the system consisting of two excitation pistons, at the second harmonic results in resonance formation $\phi^R=\pi$, and complete attenuation at $\phi^R=0$, as illustrated in Fig. 7(a). The Fig. 10 presents the instantaneous waveforms of p/p_0 and $u_1/\omega_1 l_0$ along the coordinate the coordinate x_1 ($0\le x_1\le L, x_2, x_3=0$) for one cycle of oscillations for corresponding time 160 to 161 with step $\Delta t c_s/L$=0.07 for $x_1^L=g(\omega_2,0)$, $x_1^R=g(\omega_2,\pi/10)$.

From the pressure distribution of Fig. 10(a) at $\phi^R=\pi/10$ along the pipe axis, it can be seen that the effect of the phase shift on the pressure allocation along the axis affects mainly only the reduction of the oscillation amplitude $\Delta p^*=(p_{\max}-p_{\min})/p_0$ during one period, with a pressure distribution similar to the pressure allocation at resonance, when two pressure waves converge in the middle of the pipe, and then, as a result of collision in the center of the pipe, the pressure waves diverge toward the ends of the tube. That is, when the phase shift changes, there is no strong variation in the structure of the steady state with time of a standing wave of oscillations of gas in the tube, but there is a decrease in the amplitude of oscillations. This is also confirmed by Fig. 10(b), where the distribution of particle velocities during one period of oscillation for the case $x_1^L=g(\omega_2,0)$, $x_1^R=g(\omega_2,\pi/10)$ are illustrated. The velocity allocation shows the same

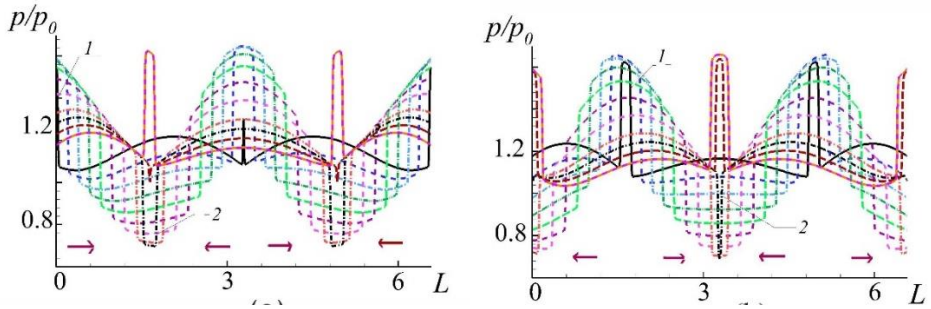

Fig. 11 Axial variations of pressure p/p_0 for $x_1^L=g(\omega_4,0)$, $x_1^R=g(\omega_4,\pi)$ along center line with a time increment of $\Delta t c_s/L=0.02$: (a) for first half-period of oscillations with dimensionless time tc_s/L from 160 to the 160.25; (b) for second half-period of oscillations from time 160.25 to the 161.5

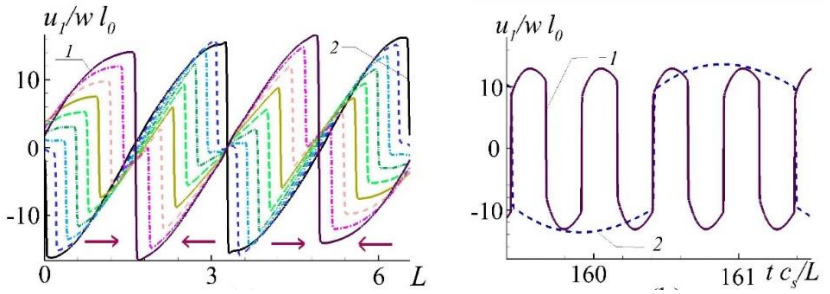

Fig. 12 Variations of axial velocity component $u_1/\omega_1 l_0$ along center line for $x_1^L=g(\omega_4,0)$, $x_1^R=g(\omega_4,\pi)$ with a time increment of $\Delta t c_s/L=0.02$ for first half-period of oscillations with dimensionless time tc_s/L from 160 to the 160.25; (b) time dependences $u_1/\omega_1 l_0$ on the time tc_s/L : 1- $x_1^L=g(\omega_4,0)$, $x_1^R=g(\omega_4,\pi)$ at point 3, 2 - $x_1^L=g(\omega_1,0)$, $x_1^R=g(\omega_1,0)$ at point 2

dynamics as in Fig. 9 (a), with a region of decreasing velocity in the middle of the tube, only if in case of resonance this region with minimum velocities for different moments of time during the period of oscillations is clearly pronounced and is located in strictly small vicinity of the tube's center, here the area is greatly enlarged, but its location does not change. Note that Fig. 10 is presented at a larger scale to more fully reflect the structure of the pressure and velocity curves, with the pressure drop Δp^* from 0.65 at resonance to 0.06 at $\phi^R=\pi/10$, and the velocity amplitude $u_1/\omega_1 l_0$ from 18.5 to 1.9.

c) Oscillations at high resonant frequencies $\omega^L=\omega^R=\omega_3,\omega_4$. Calculations carried out at higher harmonics ($\omega^L=\omega^R=\omega_3,\omega_4$) demonstrated that behavior of gas in the tube depending on phase shift ϕ^R in this case is similar to gas oscillations at lower frequencies depending on odd or even phase. The character of the oscillation amplitude as a function of ϕ^R are similar for $\omega^L=\omega^R=\omega_1$ and $\omega^L=\omega^R=\omega_3$, and for $\omega^L=\omega^R=\omega_2$ and $\omega^L=\omega^R=\omega_4$ respectively. The maximum resonance values of the vibration amplitude occur for odd harmonics, when the motion of the pistons occurs in the same phase ($\phi^L=\phi^R=0$), and for even harmonics in anti-phase ($\phi^L=\phi^R=\pi$). In the dynamics of pressure allocation along the tube axis over time for higher harmonics we can distinguish similar areas with the behavior at lower harmonics. The Fig. 11 presents the instantaneous waveforms of p/p_0 along the coordinate x_1 ($0\le x_1\le L, x_2, x_3=0$) for one cycle of oscillations for corresponding time 160 to $160\frac{1}{4}$ with step $\Delta t c_s/L=0.02$ for $x_1^L=g(\omega_4,0)$, $x_1^R=g(\omega_4,\pi)$. The feature of the p/p_0 distribution along the x_1 coordinate during the oscillation cycle for $\omega^L=\omega^R=\omega_4$ is that four weak shock waves propagate back and forth along the duct. Two high pressure zone propagates in forth direction, and two in reverse side during the first half cycle of the fluctuations period from 160 to $160\frac{1}{4}$ (Fig. 11(a)). For the second cycle of vibrations from time $160\frac{1}{4}$ to $160\frac{1}{2}$, the picture is slightly different in that, there are two areas of high pressure at the start of the report time (Fig. 11(b)) and waves are propagates in contrary side. The movement of the pressure drops along the duct Fig. 11(a)) is accompanied by a change in the velocity $u_1/\omega_1 l_0$ along the coordinate x_1 ($0\le x_1\le L, x_2, x_3=0$) for one cycle of oscillations from 160 to $160\frac{1}{4}$, as shown in Fig. 12(a). In Fig. 12(b) the time history of the velocity $u_1/\omega_1 l_0$ on the

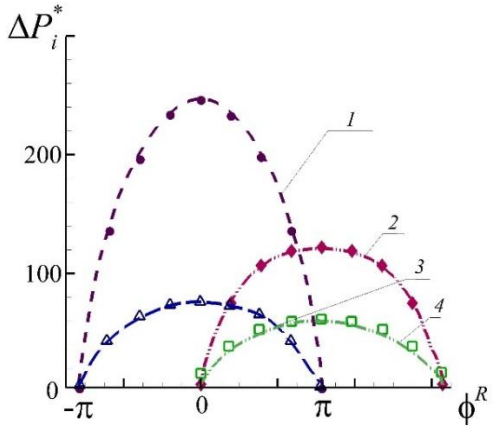

Fig. 13 Dependence of the dimensionless pressure drop $\Delta p_i^* = (p_{max} - p_{min})/(\rho_0 l_0 c_s \omega_{i=1,4})$ from phase shift ϕ^R when oscillating at different natural harmonics ω_i : 1- $\omega^L = \omega^R = \omega_1$, 2- $\omega^L = \omega^R = \omega_2$, 3- $\omega^L = \omega^R = \omega_3$, 4- $\omega^L = \omega^R = \omega_4$

dimensionless time $t c_s / L$ for $x_1^L = g(\omega_4, 0)$, $x_1^R = g(\omega_4, \pi)$ at point 3, and for $x_1^L = g(\omega_1, 0)$, $x_1^R = g(\omega_1, 0)$ at point 2 are illustrated. The feature of the velocity allocation is the transition from sinusoidal forms of velocity variation over time at harmonic oscillations to almost rectangular forms, when the smooth alteration is replaced by a jump-shaped one with the presence of some smooth section to change the direction of velocity from positive to negative (Fig. 12(b)). Calculations carried out for the oscillations in the tube under the action of two pistons at the first resonance frequency $\omega^L = \omega^R = \omega_1$ and the second resonant frequency $\omega^L = \omega^R = \omega_2$ with phase shift step $\Delta\phi = \pi/4$ has shown, that for odd (first) frequency the resonance oscillations occur at the motion of pistons on same phase $\phi^L = \phi^R = 0$, and for the even frequency (second) the resonance oscillations come at motion in anti-phase $\phi^L = \phi^R = \pi$. Accordingly, for the first resonant frequency, the oscillations are damped at shift angles equal to $\phi^R = k\pi$, $k = -1,1$, and for the second at $\phi^R = k\pi$, $k = 0, 2$. Similar behavior for the third and fourth resonant frequencies of pistons are observed. On Fig. 13 the dependence of dimensionless pressure $\Delta p_i^* = (p_{max} - p_{min})/(\rho_0 l_0 c_s \omega_{i=1,4})$ on the parameter ϕ^R for different natural frequencies of moving pistons $\omega^L = \omega^R = \omega_i, i = 1,..4$ are shown. It is observed that the dependence of pressure drop on phase shift is parabolic character, it is clear that the first natural frequency of the $\omega^L = \omega^R = \omega_1$ (Fig. 13, curve 1) near resonance ($\phi^R = 0$) large differences in pressure are observed, but with the increase of the difference of phase shift occurs a sharp decrease in amplitude. Dependence of the relative dimensionless pressure drop $\Delta p_3^* = (p_{max} - p_{min})/(\rho_0 l_0 c_s \omega_3)$ for frequency $\omega^L = \omega^R = \omega_3$ relative to ϕ^R is similar for $\omega^L = \omega^R = \omega_1$, but since the pressure drop does change very little with increasing frequency, the value of Δp_3^* decreases compared to Δp_1^*. Similar behavior for the second and fourth resonant frequencies is observed. The graph in Fig. 13 illustrates that there is a phase shift of $\Delta\phi^R = \pi$ in the formation of resonant oscillations of the gas in the tube caused by the oscillations of the two pistons at the ends for the case of even and odd harmonics. The reason for this feature will be explained at the discussion of the behavior of the wave in the gas when it approaches the right piston and reflection from it as well as with an additional impulse effect due to its mobility. Similar reasoning in wave behavior is true for the left piston, but with a slight correction. The difference in the phase shift in the formation of the resonant oscillation in the tube under the influence of two pistons at the first and second natural frequency can be seen from the pressure distributions along the pipe axis for of one period of oscillations, presented in Fig. 6(a) and Fig. 8(a), respectively. Fig.6(a) shows that the pressure wave approaches the right piston when the pressure minimum is observed here relative to mean pressure along the tube, then as a result of reflection from the piston and obtaining additional momentum there is an increase of wave energy. It occurs because the forced frequency of the piston oscillation coincides with the frequency of the gas column oscillation both in frequency and phase. As a result, we obtain an increase in the amplitude of gas oscillation. In the case of even frequency, as illustrated by Fig. 8(a), we see in this case the wave approaches the right piston with maximum pressure relative to average pressure along the pipe, and in this case additional pressure impulse from the piston to the gas column receives only when the piston moves in anti-phase in comparison with the case for the first natural frequency. The similar reasons lead to the fact that the resonant oscillations for even and odd ones occur with a phase shift of for higher harmonics (the third and fourth). The reason for the weakening of oscillations, in the case of a phase shift on the right piston let us explain for the case of oscillations at the first natural frequency. In

this case, the wave reaches the right piston, since it has a phase shift of oscillation for the right piston $\Delta\phi^R=\pi/4$, then the wave receives an additional impulse which does not coincide with the moment of reflection of the returning wave by some time interval, which leads to weakening of the additional energy to standing wave. Also, in the presence of a phase shift, the reflected and incident wave intersect, add up in amplitude, but this produces a standing wave of a smaller amplitude than at $\Delta\phi^R=0$.The standing wave amplitude for $\Delta\phi^R=\pi/4$ also increases with time, but the final steady-state amplitude value becomes smaller compared to $\Delta\phi^R=0$, as the force of the additional pressure pulses from the moving pistons becomes weaker. In this case, the structure of velocity and pressure distribution for $\Delta\phi^R=\pi/4$ remains similar, compared to with the resonant case $\Delta\phi^R=0$, but the amplitude of upgrade of pressure and velocity curves becomes smaller. A further increase in the phase shift leads to an additional weakening of the amplitude of gas oscillation in the pipe. In the case $x_1^L=g(\omega_1,0)$, $x_1^R=g(\omega_1,\pi)$ the maximum decrease amplitude of gas oscillations as a result of the superposition of incident and reflected waves at the ends of the tube from the moving pistons. In this case, over time there is a monotonic decrease in the amplitude of oscillations, resulting in that the amplitude of gas oscillations inside the tube becomes smaller than the near the moving pistons. Note the nonlinear feature depending on the differential pressure Δp_i^* from ϕ^R , which is expressed in the form of a parabolic dependence. At the initial stage variation of ϕ^R pressure drop is insignificant, and when approaching to the value of $\Delta\phi^R=\pi$ the gradient of the curve increases strongly. The calculations carried out to study the behavior of gas in the duct under impact of two pistons, oscillating at the same frequencies with phase shift showed that the amplitude of forced oscillations strongly depends on the value of phase shift. At certain values of the phase shift, nonlinear resonant oscillations develop, the magnitude of the phase shift are determined by the parity of the intrinsic harmonic value. In turn, there are values of the phase shift at which natural frequency, as well as at higher harmonics are observed. Nonlinear properties of gas behavior at resonance oscillations coincide with the peculiarities manifested at forced classical gas oscillations in a tube under the impact of only one piston, only their manifestation is stronger. The similar nonlinear characteristics in the allocation of pressure and axial velocity along the center of duct found in (Gubaidullin & Snigerev, 2022) are confirmed. For these regimes in the velocity distribution along the tube center the amplitude of velocity change remains almost unchanged, only in this case with the passage of time there is a monotonic increase of the positive velocity of the pressure front movement on the one hand, and a decrease in the negative velocity behind the pressure front on the other hand. At the same time, at the moment of collision of these two pressure fronts, there is almost equality of gas velocities from the positive and negative sides of the pressure front, then there is the reorganization the direction of movement of the pressure drop to the opposite. This dynamics of the behavior of the velocities of gas particles it is caused by the movement of pressure fronts with approximately the same amplitude towards each other, but at the moment of their collision, pressure equalization occurs along the axis of the pipe and the presence of peak pressure surges, the number of which depends on the number of the resonant harmonic. The described resonant modes arise for certain values of the phase shift, and in other cases, the presence of a phase shift leads to a monotonous attenuation of oscillations for the case of equal values of the natural frequencies of the two pistons.

3.2 Movement of Pistons at Different Natural Frequencies with Phase Shift

a) *The frequency of the left piston* $\omega^L=\omega_1$, *and the right* $\omega_{j=2,4}^R=\omega_2,\omega_3,\omega_4$ *with phase shift* .To reveal the action of the phase shift parameter ϕ^R on the character of acoustic oscillations in the tube under the action of two pistons, calculations at different angular velocities of oscillations of the left and right piston, with phase variation for the right piston were carried out. For the option under consideration, the law of oscillation on the left piston is specified as $x_1^L=g(\omega_1,0)$. At the right end, the piston vibrates harmonically with the law $x_1^R=g(\omega_{j=2,4}^R,\phi^R)$, the ω_j^R parameter takes the values $\omega_2,\omega_3,\omega_4$. The phase shift is set only for the right piston, where the parameter ϕ^R can take the following values $\phi_j^R=0,\pi/3,\pi/2,\pi$. When the system performs the previously selected number of fluctuation cycles is not enough to establish a steady standing wave in the resonator with different piston frequencies. The time when the structure will make 170 fluctuation cycles ($tc_s/2L=170$) is selected. The Fig. 14(a) shows the dynamics of pressures p/p_0 in time at point 1 for of different piston oscillations at the frequencies ω_1^L,ω_2^R: 1- $x_1^L=g(\omega_1,0)$, $x_1^R=g(\omega_2,\pi/2)$ (solid curve-1), 2- $x_1^L=g(\omega_1,0)$, $x_1^R=g(\omega_2,\pi/3)$ (dashed curve-2), 3- $x_1^L=g(\omega_1,0)$, $x_1^R=g(\omega_1,0)$ (dashed dot curve -3). In oscillations at different piston frequencies with a phase shift over time develops intense high amplitude periodic nonlinear oscillations, with formation of weak shock waves. The difference is that in this case, weaker shock waves are formed with a lower pressure jump, than at equal frequencies (Fig. 14(a), curve -3), but the difference between maximum and minimum pressure varies depending on the phase shift slightly (Fig. 14(a), curves -1,2). For comparison the nonlinear resonance oscillations of gas in tube at the equal frequencies with value ω_1 , which is illustrated by Fig. 14(a) (dashed dot curve-3) are presented. The Fig. 14(b) presents the dynamics of the time setting of the axial velocity component $u_1/\omega_1 l_0$ at point 2 for a dimensionless time tc_s/L for piston oscillations at angular frequencies ω_1^L,ω_3^R:1

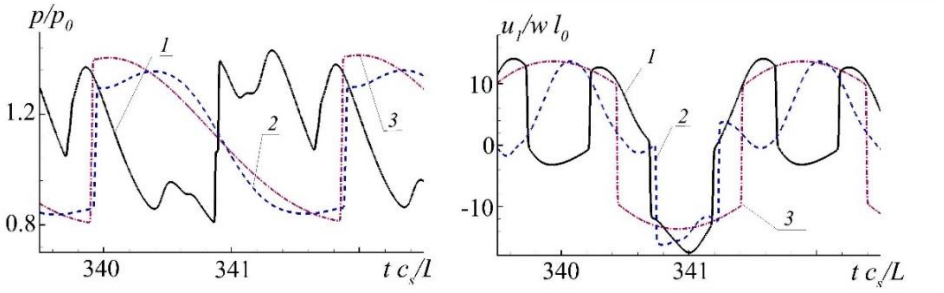

(a) (b)

Fig. 14 (a) Time dependences for p/p_0 at point 1 on the dimensionless time tc_s/L at piston vibrations at frequencies ω_1^L, ω_2^R :1- $x_1^L=g(\omega_1,0)$, $x_1^R=g(\omega_2,\pi/2)$, 2- $x_1^L=g(\omega_1,0)$, $x_1^R=g(\omega_2,\pi/3)$, 3- $x_1^L=g(\omega_1,0)$, $x_1^R=g(\omega_1,0)$; (b) Time dependences of axial velocity $u_1/\omega_1 l_0$ at piston vibrations at frequencies: 1- $x_1^L=g(\omega_1,0)$, $x_1^R=g(\omega_3,\pi/2)$, , 2- $x_1^L=g(\omega_1,0)$, $x_1^R=g(\omega_3,\pi/3)$, 3 - $x_1^L=g(\omega_1,0)$, $x_1^R=g(\omega_1,0)$

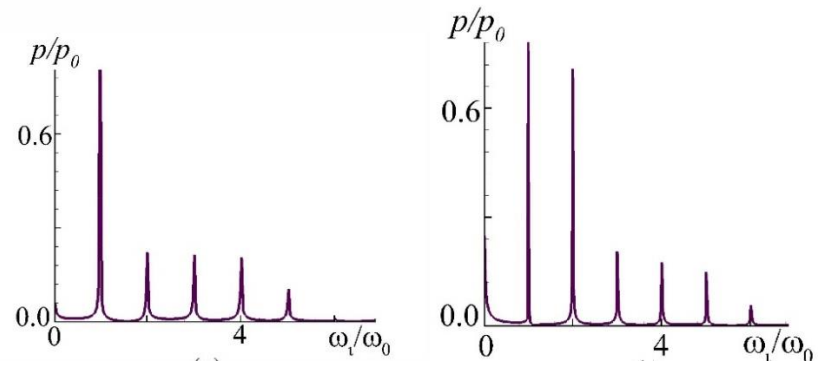

(a) (b)

Fig. 15 Fast Fourier transform of the time dependence of the pressure signal p/p_0 at the point 1($x_1/L=0.02$) for the various laws of movement of pistons: (a) $x_1^L=g(\omega_1,0)$, $x_1^R=g(\omega_2,\pi/2)$; (b) $x_1^L=g(\omega_1,0)$, $x_1^R=g(\omega_3,\pi/3)$

- $x_1^L=g(\omega_1,0)$, $x_1^R=g(\omega_3,\pi/2)$, (solid curve-1), 2- $x_1^L=g(\omega_1,0)$, $x_1^R=g(\omega_3,\pi/3)$ (dashed curve-2), 3- $x_1^L=g(\omega_1,0)$, $x_1^R=g(\omega_1,0)$ (dash dot curve-3). It can be viewed that the behavior of gas oscillations at different natural frequencies and the presence of phase shift is characterized by nonlinear oscillations of the gas, the maximum amplitude of particle velocity fluctuations does not decrease, but the value of the jump in velocity at the moments of the shock wave passes becomes less. The Fig. 15 shows a FFT of p/p_0 in time for fluctuations of gas in the tube under the action of two pistons for two variants of the laws of motion: (a) 1- $x_1^L=g(\omega_1,0)$, $x_1^R=g(\omega_2,\pi/2)$;(b) $x_1^L=g(\omega_1,0)$, $x_1^R=g(\omega_3,\pi/3)$. It can be seen that for the case when the left piston vibrates at the first natural frequency $\omega^L=\omega_1$, and the right one at higher eigenvalues $\omega_j^R=\omega_2$,then in the tube over time intense high amplitude periodic nonlinear oscillations are established, characterized by the fact, that in the spectrum of frequencies of pressure dynamics is dominated by the first natural frequency (Fig. 15(a)). In case of further increase the natural frequency of the right piston $\omega_j^R=\omega_3,\omega_4$, in the frequency spectrum of pressure, the values of the amplitudes of higher frequencies increase (Fig. 15(b)).

b) The frequency of the left piston $\omega_{j=2,3}^L=\omega_2,\omega_3$ *, and the right* $\omega_{j=3,4}^R=\omega_3,\omega_4$ *with phase shift*. Dynamics of pressure and velocity distribution during gas fluctuations in tube under the influence of two pistons at higher frequencies for one period of oscillation differs little from the case at the first resonant frequency for the left piston with a variation of frequency on the right piston. The calculations performed for the selected four phase shift values demonstrate, that in this case there is no significant decrease in oscillations depending on the phase shift and frequency change. Over time, high amplitude periodic nonlinear oscillations of the gas under the action of two pistons are established, oscillating at different natural frequencies with a phase shift. The Fig. 16(a) presents dynamics of pressures p/p_0 in time at point 1 for of different piston oscillations on the frequencies ω_2^L, ω_3^R :1- $x_1^L=g(\omega_2,0)$, $x_1^R=g(\omega_3,\pi/2)$,(solid curve -1), 2- $x_1^L=g(\omega_2,0)$, $x_1^R=g(\omega_3,\pi)$ (dashed curve-2), 3- $x_1^L=g(\omega_2,0)$, $x_1^R=g(\omega_2,\pi)$ (dash dot curve-3). The Fig. 16(b) illustrates the dynamics of the time setting of the $u_1/\omega_1 l_0$ at point 3 for a dimensionless time tc_s/L for piston oscillations at frequencies : 1- $x_1^L=g(\omega_3,0)$, $x_1^R=g(\omega_4,\pi/2)$, (solid curve-1), 2- $x_1^L=g(\omega_3,0)$,

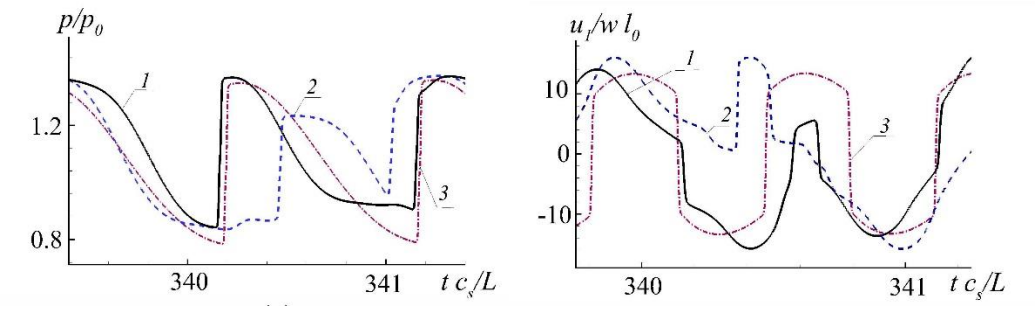

(a) (b)

Fig. 16 (a) Time dependences for p/p_0 at point 1 on the dimensionless time tc_s/L at piston vibrations at frequencies ω_2^L, ω_3^R :1- $x_1^L = g(\omega_2, 0)$, $x_1^R = g(\omega_3, \pi/2)$, 2- $x_1^L = g(\omega_2, 0)$, $x_1^R = g(\omega_3, \pi)$, 3- $x_1^L = g(\omega_2, 0)$, $x_1^R = g(\omega_2, \pi)$; (b) Time dependences of axial velocity $u_1/\omega_1 l_0$ at frequencies ω_3^L, ω_4^R :1- $x_1^L = g(\omega_3, 0)$, $x_1^R = g(\omega_4, \pi/3)$, , 2- $x_1^L = g(\omega_3, 0)$, $x_1^R = g(\omega_4, \pi/2)$, 3- $x_1^L = g(\omega_3, 0)$, $x_1^R = g(\omega_3, 0)$

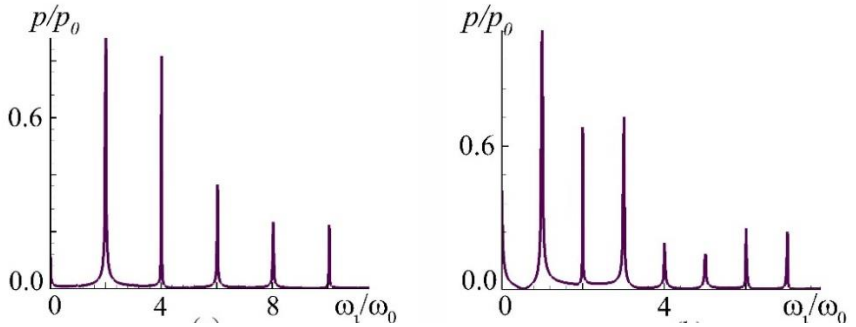

(a) (b)

Fig. 17 Fast Fourier transform of the time dependence of the pressure signal p/p_0 at the point 1 ($x_1/L = 0.02$) for the various laws of movement of pistons: (a) $x_1^L = g(\omega_2, 0)$, $x_1^R = g(\omega_3, \pi/2)$; (b) $x_1^L = g(\omega_3, 0)$, $x_1^R = g(\omega_4, \pi/3)$

$x_1^R = g(\omega_4, \pi/3)$ (dashed curve -2), 3- $x_1^L = g(\omega_2, 0)$, $x_1^R = g(\omega_2, \pi)$ (dash dot curve-3). The Fig. 17 shows a FFT of the p/p_0 in time for fluctuations of gas in the tube under the action of two pistons for two variants of the laws of motion: (a) $x_1^L = g(\omega_2, 0)$, $x_1^R = g(\omega_3, \pi/2)$;(b) $x_1^L = g(\omega_3, 0)$, $x_1^R = g(\omega_4, \pi/3)$.In the case of oscillations at higher frequencies, some features appears in the case, when both pistons operate at even frequencies. In this case, gas oscillations with a large amplitude develop in the pipe over time, and only even harmonics are present in the pressure frequency spectrum p/p_0. In the event of higher frequencies ($\omega^R = \omega_3, \omega_4$), in the tube regardless of the value of the phase shift high-amplitude oscillations are formed, in the pressure spectrum p/p_0 all harmonics are present, the amplitudes of which may have different (not necessarily decreasing) values. The calculations carried out to study the behavior of gas in a pipe under the influence of two pistons oscillating at different frequencies with a phase shift showed that the amplitude of the forced oscillations does not depend much on the value of the phase shift ϕ^R . In the selected range of changes in the phase shift ϕ^R of the right piston, calculations have shown, that there is no any attenuation of fluctuations over time are observed. The effect of the phase shift ϕ^R in gas oscillations in a system consisting of two excitation pistons, at different frequencies does not lead to a significant decrease in the amplitude of the steady-state gas oscillations in the tube. The Fig. 18 demonstrates the more detail distributions of the gas p/p_0 and $u_1/\omega_1 l_0$ along the duct for one cycle of fluctuations with motion of pistons with law $x_1^L = g(\omega_3, 0)$, $x_1^R = g(\omega_4, \pi/3)$. From the figure of pressure allocation we see that in the steady-state mode of oscillations in the tube, although the pistons move at the second and third harmonics, for one period of steady state of periodic oscillations in the tube moves only one jump of pressure, which amplitude is lower than for resonance case. Which indicates that the predominant time-varying signal alteration for pressure is the first frequency, on which the pressure changes at higher harmonics are superimposed. The velocity allocation curves also show that along the axis is closer to in structure to oscillations at the first resonant frequency, characterized by the presence of only one maximum velocity value along the tube axis. From the pressure distribution we can see that the first frequency is the predominant in the frequency spectrum of the pressure signal, which is presented in Fig. 15 and Fig. 17, obtained using the fast Fourier transform. But at some moments of time for the period the pressure decrease along the axis is equal in amplitude to the pressure drop for the resonant case (for equal frequencies of pistons), therefore the amplitudes of changes of velocity of gas particles are also close to the resonant ones. The difference of pressure distributions for the case of gas oscillations at different

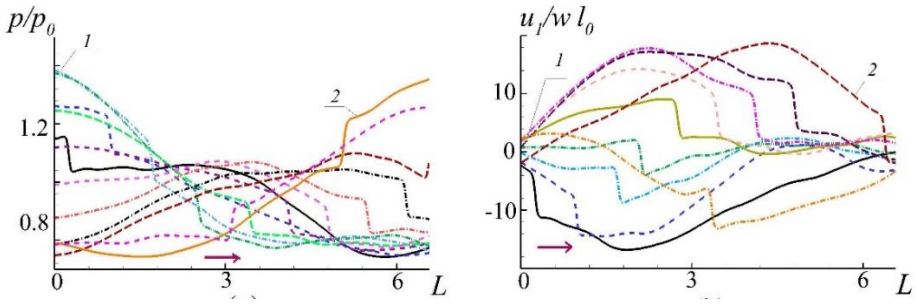

(a) (b)

Fig. 18 Axial variations of variables for $x_1^L = g(\omega_3, 0)$, $x_1^R = g(\omega_4, \pi/3)$ **with a time increment of** $\Delta t c_s / L = 0.08$ **for period of oscillations for dimensionless time** $t c_s / L$ **from 341 to the 342: (a) pressure** p/p_0 **; (b) axial velocity component** $u_1 / \omega_1 l_0$.

frequencies is that the significant pressure drop is distributed more uniformly along the entire length of the pipe, leading to the fact that maximum velocities at some moments of time are also observed in the pipe region, but the gradient of velocity alteration along the length varies smoothly. Similar pressure and velocity allocations are observed for all selected discrete values. The same pressure and velocity allocations are observed for all selected discrete phase shift values, which leads to the fact that over time for all values of ϕ^R the significant oscillations of the gas in the tube with a complex standing wave form are established. The reason that the oscillation of the gas in the tube under the influence of two pistons, oscillating at different natural frequencies does not lead to noticeable damping of oscillations, it that the incident waves of longer length are reflected from the right piston, oscillating at a higher frequency with a phase shift. The additional pulses from the right-hand piston, however, lead to the formation of waves of shorter length, which intersect and add up with waves of larger length with a phase shift, but eventually the interference of waves leads to amplification of longer waves. Over time, regardless of the value of the phase shift at the higher frequency piston, as a result of interference there is an increase of amplitude of longer waves and formation of a standing wave with high amplitude in oscillations of gas in the pipe.

4. CONCLUSION

The nonlinear effects in fluctuations of gas in duct forced by two pistons at first and higher modes with phase shift are observed. The analysis of the calculations of a resonator excited by two pistons oscillating at different natural frequencies and having a phase shift has demonstrated, that the effect of phase shift changes on the character of acoustic oscillations has some characteristic features. The effect of the phase shift value has a strong effect on the oscillation amplitude at pistons oscillating at equal natural frequencies, in turn, when the pistons oscillate at different natural frequencies, the effect is very small. The dependence of dimensionless maximum pressure drop amplitude on phase shift at pistons operation at equal frequencies has a parabolic character, at that, with the increase of frequency of piston motion the gradient of the curve of dependence the difference pressure from the phase shift decreases, and the radius of curvature of the parabolic curve increases and it becomes smoother. Also in the tube there are forced gas oscillations of large amplitude leading to weak shock waves at operation of pistons at equal natural frequencies in one phase at odd values of harmonics, and in operation in anti-phase at even values of harmonics. The influence of phase shift in the movement of pistons at equal frequencies also manifested in the fact, that at certain values of the phase shift there is a strong attenuation of the oscillations. Numerical analysis illustrated that induced acoustic vibrations in the tube during the operation of two pistons oscillating on different phase-shift frequencies are characterized by significant amplitudes of pressure and velocity drops, values of which differ from resonant values at equal frequencies not more than 6-9 % percent. In the considered variants of calculations, when varying natural frequencies and phase shifts, no cases with significant attenuation of oscillations are observed.

ACKNOWLEDGEMENTS

This study was performed by a grant from the Russian Science Foundation (project no. 20–11–20070, https://rscf.ru/en/project/20-11-20070).

CONFLICT OF INTEREST

The author(s) declared no potential conflicts of interest with respect to the research, authorship and publication of this article.

AUTHORS CONTRIBUTION

All authors contributed to the conceptualization and methodology. Damir Gubaidullin: project administration, resources, funding acquisition. Boris Snigerev: writing-original draft, writing review and editing, software, visualization, investigation. All authors read and revised the final manuscript.

REFERENCES

Aganin, A. A., Ilgamov, M. A., & Smirnova, E. T. (1996). *Journal of Sound and Vibration,* 195, 359-374.

https://doi.org/10.1006/jsvi.1996.0431

Alexeev, A., & Gutginger, C. (2003). Resonance gas oscillations in closed tubes: Numerical study and experiments. *Physics of Fluids,* 15, 3397-3408. https://doi.org/10.1016/j.ultsonch.2018.05.011

Antao, D. S., & Farouk, B. (2013). High amplitude nonlinear wave driven flow in cylindrical and conical resonators. *Journal of the Acoustical Society of America,* 134, 917-932. https://doi.org/10.1121/1.4807635

Backhaus, S., & Swift, G. W. (1999). A Thermoacoustic Stirling heat engine. *Nature,* 339, 335-338. https://doi.org/10.1038/20624

Bearman, P. W., & Obasaju, E. D. (1982). An experimental study of pressure fluctuations on fixed and oscillating square-section cylinders. *Journal of Applied Fluid Mechanics,* 119, 297–321. https://doi.org/10.1017/S0022112082001360

Carpinlioglu, M. O., & Gundogdu, M. Y. (2001). A critical review on pulsatile pipe flow studies directing towards future research topics. *Flow Measurement and Instrumentation,* 12, 163-174. https://doi.org/10.1016/S0955-5986(01)00020-6

Chester, W. (1963). Resonant oscillations in closed tubes. *Journal of Fluid Mechanics*, 18, 44-64. https://doi.org/10.1017/s0022112064000040.

Chun, Y. D., & Kim, Y. H. (2000). Numerical analysis for nonlinear resonant oscillations of gas in axisymmetric closed tubes. *Journal of the Acoustical Society of America,* 108, 2765-2774. https://doi.org/10.1121/1.1312363

Colonius, T., & Lele, K. (2004). Computational aeroacoustics: Progress on nonlinear problems of sound generation. *Progress in Aerospace Sciences,* 40, 345-416. https://doi.org/10.1016/j.paerosci.2004.09.001

Cruikshank, D. B. (1972). Experimental investigation of finite-amplitude acoustic oscillations in a closed tube. *Journal of the Acoustical Society of America,* 52, 1024-1036. https://doi.org/10.1121/1.1913171

Gubaidullin, D. A., & Snigerev, B. A. (2022). Numerical simulation of forced acoustic gas oscillations with large amplitude in closed tube. *Wave Motions,* 112, 102941. https://doi.org/10.1016/j.wavemoti.2022.102941

Hossain, M. A., Kawahashi, M., & Fujioka T. (2005). Finite amplitude standing wave in closed ducts with cross sectional area change. *Wave Motions,* 42, 226-237. https://doi.org/10.1016/j.wavemoti.2005.02.003

Ilinskii,Y. A., Lipkens, B., Lucas, T. S., Van Doren, T. W., & Zabolotskaya, E. A. (1998). Nonlinear standing waves in an acoustical resonator. *Journal of the Acoustical Society of America,* 104, 2664-2674. https://doi.org/10.1121/1.423850

Kinsler, L. E., Frey, A. R., Coppens, A. B., & Sanders, J. V. (1999). *Fundamentals of Acoustics.* Wiley, New York.

Kraposhin, M. V., Banholzer, M., Pfitzner, M., & Marchevsky, I. K. (2018). A hybrid pressure-based solver for nonideal single-phase fluid flows at all speeds. *International Journal of Numerical Methods in Fluids,* 88, 79-99. https://doi.org/10.1002/fld.4512

Kraposhin, M. V., Bovtrikova, A., & Strijhak, S. (2015). Adaptation of Kurganov-Tadmor numerical scheme for applying in combination with the piso method in numerical simulation of flows in a wide range of Mach numbers. *Procedia Computer Science,* 66, 43-52. https://doi.org/10.1016/j.procs.2015.11.007

Lawrenson, C. C., Lipkens, B., Lucas, T. S., Perkins, D. K., & Van Doren, T. W. (1998). Measurements of macrosonic standing waves in oscillating closed cavities. *Journal of the Acoustical Society of America* 104, 623-636. https://doi.org/10.1121/1.423306

Li, G., Zheng, Y., Yang, H., & Xu, Y. (2016). Numerical investigation of heat transfer and fluid flow around the rectangular flat plane confined by a cylinder under pulsating flow. *Journal of Applied Fluid Mechanics,* 9, 1569 - 1577. https://doi.org/10.18869/acadpub.jafm.68.235.24140

Marie, S., Ricot, D., & Sagaut, P. (2009). Comparison between lattice boltzmann method and Navier–stokes high order schemes for computational aeroacoustics. *Journal of Computaional Physics,* 228, 1056-1070. https://doi.org/10.1016/j.jcp.2008.10.021

Mithun, M. G., Kumar, P. & Tiwari, S. (2018). Numerical investigations on unsteady flow past two identical inline square cylinders oscillating transversely with phase difference. *Journal of Applied Fluid Mechanics* 11, 847-859. https://doi.org/10.29252/jafm.11.04.28314

Moukalled, F., Mangani, M., & Darwish, L. (2001). *The finite volume method.* computational fluid dynamics. An Advanced Introduction with OpenFOAM and Matlab. Springer Verlag, Berlin. https://doi.org/10.1007/978-3-319-16874-6

Ning, F., & Li X. (2013). Numerical simulation of finite amplitude standing waves in acoustic resonators using finite volume method. *Wave Motions,* 50, 135-145. https://doi.org/10.1016/j.wavemoti.2012.08.001

Ohmi, M., & Iguchi, M. (1982). Critical Reynolds number in an oscillating pipe flow. *Bulletin of the Japan Society of Mechanical Engineers* 25, 8-9. https://doi.org/10.1299/jsme1958.25.165

Penelet, G., Guedra, M., Gusev, V., & Devaux, T. (2012). Simplified account of Rayleigh streaming for the description of nonlinear processes leading to steady state sound in thermoacoustic engines. *International Journal of Heat and Mass Transfer*, 55, 6042-6053. https://doi.org/10.1016/j.ijheatmasstransfer.2012.06.015

Pillai, A. V., & Manu, K. V. (2020). Analytical solutions for unsteady pipe flows with slip boundary condition. *Journal of Applied Fluid Mechanics,* 13, 1015–1026.

https://doi.org/10.29252/jafm.13.03.30800

Piscaglia, F., Montorfano A., & Onorati, A. (2013). Development of a non-reflecting boundary condition for multidimensional nonlinear duct acoustic computation, *Journal of Sound and Vibration,* 332, 922-935. https://doi.org/10.1016/j.jsv.2012.09.030

Saenger, R., & Hudson, G. (1960). Periodic shock waves in resonating gas column. *Journal of the Acoustical Society of America,* 32, 961-967. https://doi.org/10.1121/1.1908343

Singh, N. K., & Rubini, P. A. (2015). Large eddy simulation of acoustic pulse propagation and turbulent flow interaction in expansion mufflers. *Applied Acoustics* 98, 6-19. https://doi.org/10.1016/j.apacoust.2015.04.015

Swift, G. W. (1992). Analysis and performance of a large thermoacoustic engine. *Journal of the Acoustical Society of America,* 92, 1551-1563. https://doi.org/10.1121/1.403896

Thomas, S. K., & Muruganandam, T. M. (2018). A Review of acoustic compressors and pumps from fluidics perspective. *Sensors and Actuators A: Physical,* 183, 43-53. https://doi.org/10.1016/j.paerosci.2004.09.001

Vanhille, C., & Campos-Pozuelo, C. (2001). Numerical model for nonlinear standing waves and weak shocks in thermoviscous fluids. *Journal of the Acoustical Society of America,* 109, 2660-2667. https://doi.org/10.1121/1.423850

Wang, J., Dixia F., & Lin, K. (2020). A review on flow-induced vibration of offshore circular cylinders. *Journal of Hydrodynamics,* 32, 415-440. https://doi.org/ 10.1007/s42241-020-0032-2

Wang, M., Freund, J. B., & Lele, K. (2006). Computational prediction of flow-generated sound. *Annual Review of Fluid Mechanics,* 38, 483-512. https://doi.org/10.1146/annurev.fluid.38.050304.092036

Weller, H. G., Tabor, G., Jasak, H., & Fureby C. (1998). A tensorial approach to computational continuum mechanics using object-oriented techniques, *Computers in Physics,* 12, 620-631. https://doi.org/10.1063/1.168744

Zaripov, R. G., & Ilhamov, M. A. (1976). Non-linear gas oscillations in a pipe. *Journal of Sound and Vibration* 46, 245-257. https://doi.org/10.1016/0022-460x(76)90441-7